PHYSICAL REVIEW B **93**, 241403(R) (2016)

Energy gaps of atomically precise armchair graphene sidewall nanoribbons

Wen-Xiao Wang,[1] Mei Zhou,[2] Xinqi Li,[3] Si-Yu Li,[1] Xiaosong Wu,[3] Wenhui Duan,[2] and Lin He[1,*]

[1]*Center for Advanced Quantum Studies, Department of Physics, Beijing Normal University, Beijing, 100875, People's Republic of China*

[2]*State Key Laboratory of Low-Dimensional Quantum Physics and Collaborative Innovation Center of Quantum Matter, Department of Physics, Tsinghua University, Beijing, 100084, People's Republic of China*

[3]*State Key Laboratory for Artificial Microsctructure and Mesoscopic Physics, Peking University, Beijing 100871, China and Collaborative Innovation Center of Quantum Matter, Beijing 100871, China*

(Received 3 February 2016; revised manuscript received 8 May 2016; published 9 June 2016)

Theoretically, it has been demonstrated that armchair Graphene nanoribbons (GNRs) can be divided into three families, i.e., $N_a = 3p$, $N_a = 3p + 1$, and $N_a = 3p + 2$ (here N_a is the number of dimer lines across the ribbon width and p is an integer), according to their electronic structures, and the energy gaps for the three families are quite different even with the same p. However, a systematic experimental verification of this fundamental prediction is still lacking, owing to very limited atomic-level control of the width of the armchair GNRs investigated. Here, we studied electronic structures of the armchair GNRs with atomically well-defined widths ranging from $N_a = 6$ to $N_a = 26$ by using a scanning tunneling microscope. Our result demonstrated explicitly that all the studied armchair GNRs exhibit semiconducting gaps and, more importantly, the observed gaps as a function of N_a are well grouped into the three categories, as predicted by density-functional theory calculations. Such a result indicated that the electronic properties of the armchair GNRs can be tuned dramatically by simply adding or cutting one carbon dimer line along the ribbon width.

DOI: 10.1103/PhysRevB.93.241403

Graphene nanoribbons (GNRs) are one-dimensional (1D) structures that exhibit a rich variety of electronic properties [1–17]. Therefore, they are predicted to be the building blocks in next-generation nanoelectronic devices. Theoretically, it was well established that the electronic structures of GNRs are strongly dependent on their widths and edge orientation [1–6]. For example, the energy gaps of the armchair GNRs sensitively depend on the number of dimer lines N_a along the ribbon width, as shown in Fig. 1 (see Supplemental Material for details of first principles calculations [18]). For the three different categories with $p = 5$, the armchair GNRs with $N_a = 15(N_a = 3p)$ and $N_a = 16(N_a = 3p + 1)$ display energy gaps $E_g = 556$ meV and $E_g = 657$ meV, respectively, whereas the armchair GNR with $N_a = 17(N_a = 3p + 2)$ is predicted to exhibit a much smaller gap $E_g = 118$ meV [Fig. 1(b)]. Because of the highly tuneable feature of their electronic properties, armchair GNRs are believed to be one of the most promising candidates toward the design of graphene-based circuits for technological applications. This stimulates the development of many different methods in fabricating high-quality GNRs [10,12,13,17,19–22]. However, the studied armchair GNRs with atomically well-defined widths and edge orientation are rather limited up to now [13,17,21,22]. A rare example is the observation of about 100-meV bandgap in a $N_a = 5$ armchair GNR (the length of the studied GNR is about 5 nm), which really indicates that the $N_a = 3p + 2$ (here $p = 1$) armchair GNR should exhibit a very small bandgap [17]. Very recently, STM study of armchair GNRs with widths ranging from about 3.5 ± 0.5 nm to 10.5 ± 0.5 nm revealed that these GNRs can be grouped into two families: one displays large gaps, which is attributed to the ribbons belonging to the $N_a = 3p$ and $N_a = 3p + 1$ classes; the other exhibits no detectable gap, which is attributed to the ribbons belonging to the $N_a = 3p + 2$ class [13]. This result is clearly indicative of width-dependence physics in the armchair GNRs; however, the lack of exact number of carbon dimer lines N_a across the width of these GNRs, owing to the measurement error and the atomic-scale edge irregularities [13], did not allow a more systematic insight.

To experimentally verify the width-dependence physics in the armchair GNRs, we realized the growth of 0.6- to 3.1-nm-wide armchair GNRs with well-defined $N_a(6 \leqslant N_a \leqslant 26)$ on the nanometer-wide C-face terraces of SiC (see Supplemental Material [18] for details) [23–25], as schematically shown in Fig. 2(a). These ultranarrow sidewall GNRs provide us unprecedented opportunities to address this issue and, moreover, our scanning probe technique allows us to directly measure the energy gaps and the exact N_a of these GNRs simultaneously. Previously, the growth of GNRs on the slope of a Si-face terraced SiC surface with crystallographically perfect edges was reported [14–16]. These GNRs are usually of several tens of nanometers and the boundaries of the GNRs are defined by regions where they attach to graphene tightly bonded to the (0001) oriented terraces (in these terraces, the carbon atoms are strongly bonded to the exposed Si atoms of SiC), i.e., the so-called graphene buffer layer of Si-face of SiC [14,15]. It has been demonstrated that the GNRs on the slope are decoupled from the substrate and behave as free-standing ribbons with similar widths [14–16]. Very recently, 1- to 2-nm-wide GNRs decoupled from the substrate were further observed on the sidewall between the (0001) oriented nanoterraces of SiC [16]. Our experimental result, as shown in Fig. 2, demonstrates that similar ultranarrow GNRs could also be formed on the C-face nanoterraces of SiC.

The scanning tunneling spectroscopy (STS) measurements in Fig. 2(c) indicate that graphene sheet in the C-face large-scale terraces [with the width of a few hundreds of nanometers, as shown in Fig. 2(b)] is decoupled from the substrate, as reported previously (see Supplemental Material [18] for

*helin@bnu.edu.cn

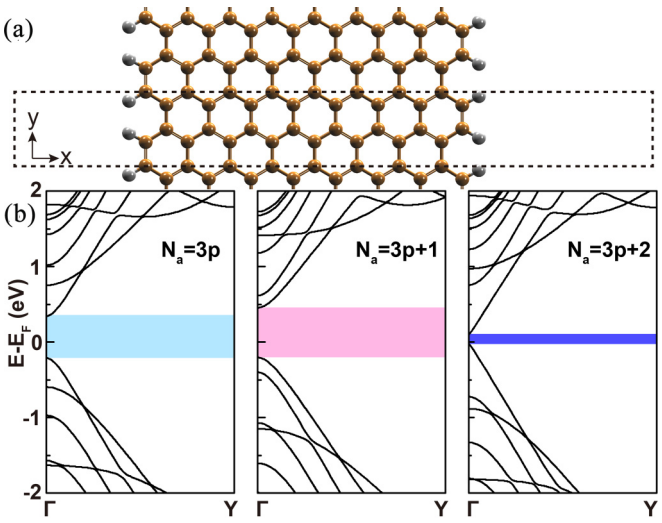

FIG. 1. Geometry and electronic structure of armchair GNRs. (a) Schematic of a $N_a = 15$ armchair GNR with the edge dangling σ bonds passivated by hydrogen atoms (gray balls). Black dashed frame indicates the supercell in the calculation. (b) Band structures of N_a armchair GNRs with $N_a = 3p, 3p+1$, and $3p+2$ (here $p = 5$) obtained by first-principles calculations. The colored areas indicate the energy bandgaps of the three different families of the armchair GNRs. Obviously, the $N_a = 3p+2$ armchair GNR exhibits a much smaller bandgap.

details of STM measurements). The spectra of the graphene sheet, recorded in the magnetic field of 4 T, exhibit Landau quantization of massless Dirac fermions (with the hallmark zero-energy Landau level and its characteristic nonequally spaced energy-level spectrum of Landau levels), as expected to be observed in a pristine graphene monolayer [26–29]. In between the C-face nanoterraces (with the width of only a few nanometers), the graphene is strongly bonded to the substrate, i.e., the exposed Si atoms of SiC, and behaves as the graphene buffer layer. The profile line across the C-face nanoterraces [Fig. 2(f)] directly demonstrated that the free-standing graphene regions on the nanoterraces and the pinning regions on the sidewall are quite different, owing to their different coupling strengths with the substrate. The spatial variation of the interaction with the substrate can change the electronic properties of graphene dramatically [14–16,30]. The ultranarrow armchair GNRs on the C-face nanoterraces, as shown in Figs. 2(d) and 2(e), are expected to exhibit energy gaps due to quantum confinement. Theoretically, the energy gaps of these decoupling armchair GNRs on SiC surface, obtained by first-principle calculations, are on the order of magnitude of the expected gaps for free-standing armchair GNRs with similar widths [16]. In our experiment, the widths of the armchair GNRs, i.e., the number of carbon dimer lines across the ribbons width, can be determined exactly according to the atomic-resolution STM images [Fig. 2(e)] and the profile line across the ribbons [Fig. 2(f)]. The STS spectra recorded across the ribbons, as shown in Fig. S1 of Ref. [18], for an example, help us to further confirm the edges of the ribbons. After carefully examining hundreds of C-face nanoterraces on SiC surface, we obtain armchair GNRs with different widths and the measured value of N_a ranges from $N_a = 6$ to $N_a = 26$. Therefore, these armchair GNRs provide an attractive platform

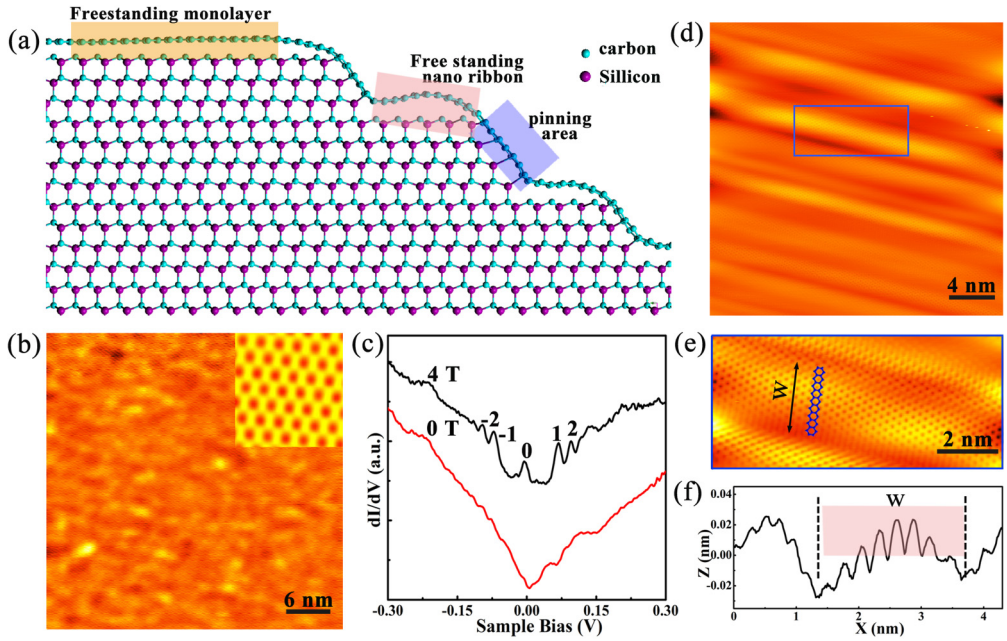

FIG. 2. Structures of graphene and GNRs on C-face terraces of SiC surface. (a) Schematic structure of graphene monolayer on C-face terraces of SiC surface. There are three different regions exhibiting quite different electronic properties. (b) A representative STM image of a graphene sheet on a C-face terrace of SiC surface ($V_{\text{sample}} = -0.9$ V, $I = 0.28$ nA). The inset shows an atomic-resolution STM image of the graphene sheet. (c) STS spectra, i.e., *dI/dV-V* curves, taken at the position in panel (b) under zero and 4 T magnetic fields. For clarity, the curves are offset on the y axis and Landau level indices of massless Dirac fermions are marked. (d) A typical STM image ($V_{\text{sample}} = 0.8$ V, $I = 0.3$ nA) showing a graphene sheet across several adjacent C-face nanoterraces of SiC surface. The atomic-resolution STM image of an armchair GNR on a C-face nanoterrace is shown in panel (e). The atomic structure of graphene is overlaid onto the STM image to determine the number of carbon dimer lines along the ribbon width. (f) A profile line across the GNR width.

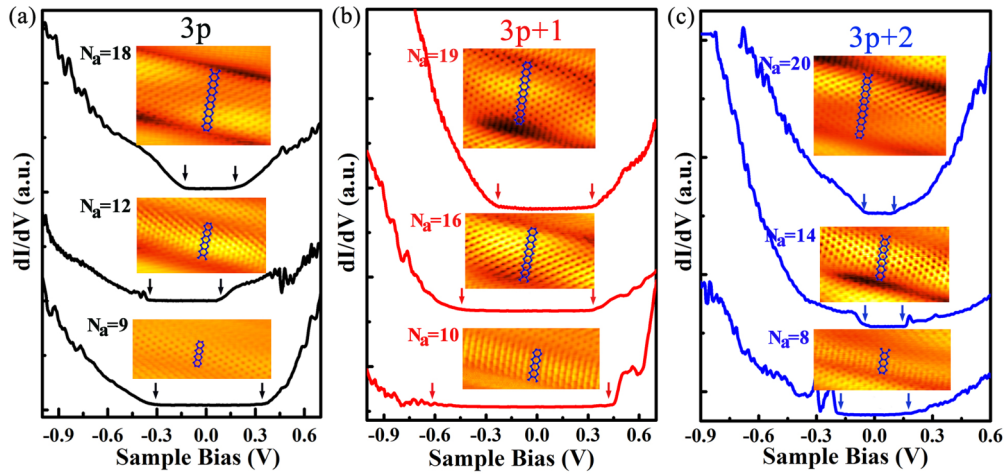

FIG. 3. STS spectra of armchair GNRs with different widths on C-face nanoterraces of SiC surface. Representative spectra of different armchair GNRs belonging to the (a) $N_a = 3p$, (b) $N_a = 3p + 1$, and (c) $N_a = 3p + 2$ families. The corresponding atomic-resolution STM images of these armchair GNRs are shown in the insets. The edges of the energy bandgap of the STS spectra are marked by two arrows. The peaks in the spectra are the van Hove singularities induced by 1D electron confinement.

to explore the highly tunable semiconductor bandgaps, which are simply determined by the value of N_a, in the armchair GNRs.

Figure 3 shows several representative STS spectra of the armchair GNRs with different N_a. Obviously, all the studied armchair GNRs exhibit semiconducting gaps. For clarity, we plotted the spectra according to the three categories of the widths of the armchair GNRs. For each category, the energy gaps of the GNRs decrease with increasing N_a, as expected to be observed due to the quantum confinement. A notable feature of the spectra is that the $N_a = 3p + 2$ armchair GNRs display a much smaller gap comparing to that of the other two categories. Such a result demonstrated directly that the energy bandgaps of the armchair GNRs depend sensitively on the value of N_a. Theoretically, the opening of small bandgaps in the $N_a = 3p + 2$ armchair GNRs is closely related to edge distortion due to hydrogen passivation of the edges [3,31]. In our experiment, the strong bonding to the exposed Si atoms of SiC could also lead to edge distortion and, consequently, result in the gap opening of the $N_a = 3p + 2$ armchair sidewall GNRs. The slight deviation between the experiment and the theory for the $N_a = 3p + 2$ armchair GNRs may arise from different edge distortions.

To further explore the electronic properties of the GNRs, we carried out measurements of the spatially resolved tunneling spectra along the ribbons. For an armchair GNR with a fixed N_a, it exhibits an almost constant energy bandgap, as shown in Fig. 4(a), for an example. However, in some of the armchair GNRs on SiC surface, spatially resolved tunneling spectra, as shown in Figs. 4(b) and 4(c), for examples, reveal that the energy gaps vary spatially along the ribbon. Such a result is attributed to the width-dependent energy gaps of the armchair GNRs. For the nanometer-wide armchair ribbons, the energy gaps vary a lot, even when we only change one carbon dimer line across the ribbon width, as shown in Fig. 4(c). This behavior not only provides us unprecedented control over electronic properties of the graphene GNRs at atomic-level, but also opens the way toward the realization of electronic

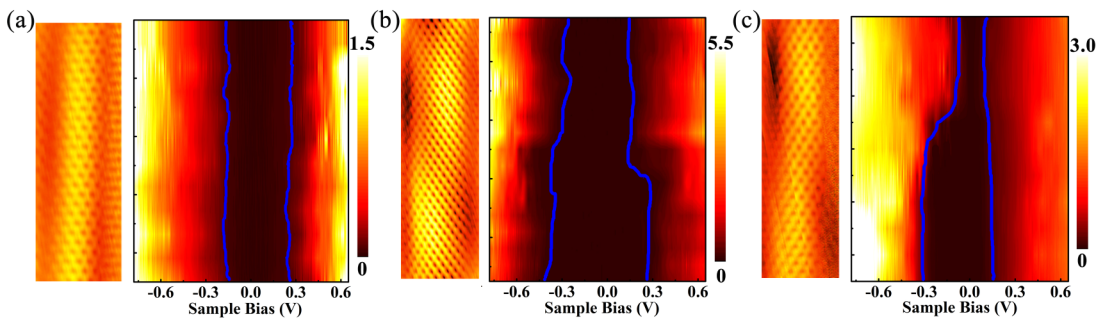

FIG. 4. Spatially resolved band gaps of three armchair GNRs by tunnelling spectroscopy. (a) Left: Atomic resolution STM image of an armchair GNR with $N_a = 3p + 2 = 8$. Right: Intensity plot of *dI/dV* spectra taken along the armchair GNR. The armchair GNR exhibits a constant bandgap along it. (b) Left: Atomic resolution STM image of an armchair GNR showing a transition of widths from $N_a = 3p = 15$ (top) to $N_a = 3p + 1 = 16$ (bottom). Right: Intensity plot of *dI/dV* spectra taken along the armchair GNR exhibiting a variation of the gaps from about 428 to 661 meV along it. (c) Left: Atomic resolution STM image of an armchair GNR showing a transition of widths from $N_a = 3p + 2 = 11$ (top) to $N_a = 3p = 12$ (bottom). Right: Intensity plot of *dI/dV* spectra taken along the armchair GNR exhibiting a large variation of the gaps from about 150 to about 445 meV along it. The edges of bandgap are highlighted with blue lines in the spectra maps.

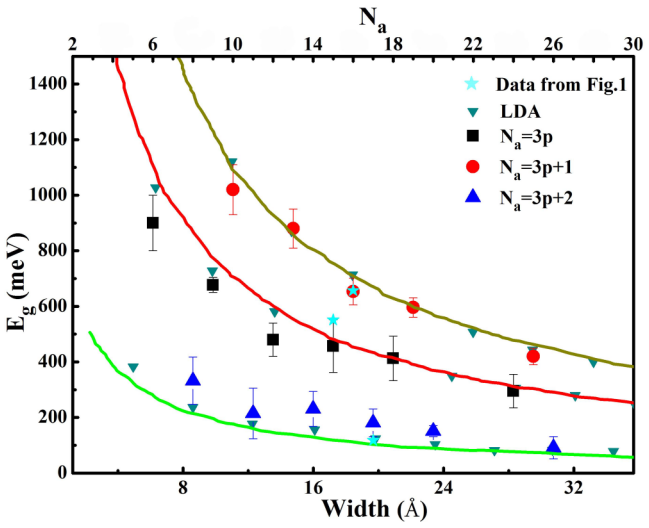

FIG. 5. The measured bandgap of the armchair GNRs as a function of widths. The measured energy bandgaps can be grouped into three categories. The theoretical data points taken from Ref. [3] are also given for comparison. The solid lines are calculated according to Eq. (1) of Ref. [3].

junctions entirely in a GNR. In the experiment, we observed that the change in the bandgap of the armchair GNR is smoother than that of the nanoribbon width (Fig. 4). Similar result has also been observed previously in zigzag GNRs with nonuniform widths [12]. Such a behavior indicates that the electronic structures around the conjunct boundary of the two adjacent GNRs with different widths differ much from that of the two adjacent GNRs and the bandgap changes smoothly across the boundary. The length of the transition region for the bandgaps is about 1–2 nm.

Figure 5 summarized the energy bandgaps E_g of the studied armchair GNRs as a function of N_a. Here we should point out that we only summarized the result of the armchair GNRs with uniform widths over several tens of nanometers. The observed gaps as a function of N_a can be well grouped into the three categories. The $E_g \sim N_a^{-1}$ behavior for all the three categories further confirms that the origin of the energy gaps for GNRs with armchair edges is the quantum confinement. The energy gaps of freestanding armchair GNRs with different widths obtained by first-principles theoretical calculations [3] are also plotted for comparison. Obviously, the theoretical result reproduces the overall features of the observed width-dependent energy gaps for the armchair GNRs on SiC surface. In the LDA calculations (as shown in Fig. 1 and as reported in Ref. [3]), the edges of the nanoribbons are passivated with H atoms and the electron-electron interactions are ignored. In our experiment, the quantum confinement of the armchair sidewall GNRs arises from the strong bonding of graphene to the exposed Si atoms of SiC. It is still expected that the armchair sidewall nanoribbons can be grouped into three categories. However, there are many obvious differences between the experiment and the theoretical model. Therefore, the good agreement between the experiment and the gaps obtained by LDA calculations is quite surprising. However, we should point out that our experimental result also agrees with previous theoretical calculations on the armchair GNRs with taking into account the SiC surface [16]. In our experiment, the observed gaps of the armchair sidewall GNRs, as shown in Fig. 5, are much smaller than the predicted *GW* gaps of free-standing GNRs [5]. The main reason for this deviation may arise from the fact that the armchair sidewall GNRs are generated by the strong bonding of graphene to the exposed Si atoms of SiC. Such a "chemical cutting" of the sidewall GNRs differs much from the "physical cutting" of real freestanding GNRs.

In summary, we measured energy gaps of atomically precise armchair graphene sidewall nanoribbons with widths ranging from $N_a = 6$ to $N_a = 26$. We demonstrated that all the armchair GNRs exhibit semiconducting gaps due to quantum confinement and the GNRs are well grouped into three categories according to their electronic structures. Our result indicated that the electronic structures of the armchair GNRs can be tuned dramatically by simply adding or cutting one dimer line along the ribbon width.

This work was supported by the National Basic Research Program of China (Grants No. 2014CB920903 and No. 2013CBA01603), the National Natural Science Foundation of China (Grants No. 11422430, No. 11374035, No. 11334006, and No. 11222436), the program for New Century Excellent Talents in University of the Ministry of Education of China (Grant No. NCET-13-0054), Beijing Higher Education Young Elite Teacher Project (Grant No. YETP0238). L.H. also acknowledges support from the National Program for Support of Top-notch Young Professionals. The first principles calculations were performed on the "Explorer 100" cluster system at Tsinghua University.

[1] K. Nakada, M. Fujita, G. Dresselhaus, M. S. Dresselhaus, Edge state in graphene ribbons: Nanometre size effect and edge shape dependence. Phys. Rev. B **54**, 17954 (1996).

[2] Y.-W. Son, M. L. Cohen, S. G. Louie, Half-metallic graphene nanoribbons. Nature **444**, 347 (2006).

[3] Y.-W. Son, M. L. Cohen, S. G. Louie, Energy Gaps in Graphene Nanoribbons. Phys. Rev. Lett. **97**, 216803 (2006).

[4] V. Barone, O. Hod, G. E. Scuseria, Electronic structure and stability of semiconducting graphene nanoribbons. Nano Lett. **6**, 2748 (2006).

[5] L. Yang, C.-H. Park, Y.-W. Son, M. L. Cohen, S. G. Louie, Quasiparticle Energies and Band Gaps in Graphene Nanoribbons. Phys. Rev. Lett. **99**, 186801 (2007).

[6] O. V. Yazyev, A guide to the design of electronic properties of graphene nanoribbons. Acc. Chem. Res. **46**, 2319 (2013).

[7] M. Y. Han, B. Ozyilmaz, Y. Zhang, and P. Kim. Energy Band-Gap Engineering of Graphene Nanoribbons. Phys. Rev. Lett. **98**, 206805 (2007).

[8] Q. Yan, B. Huang, J. Yu, F.-W. Zheng, J. Zang, J. Wu, B.-L. Gu, F. Liu, and W.-H. Duan, Intrinsic current-voltage characteristics

of graphene nanoribbon transistors and effect of edge doping. Nano Lett. **7**, 1469 (2007).

[9] X. Wang, Y. Ouyang, L. Jiao, H. Wang, L. Xie, J. Wu, J. Guo, H. Dai, Graphene nanoribbons with smooth edges behave as quantum wires. Nature Nano. **6**, 563 (2011).

[10] L. Tapaszto, G. Dobrik, P. Lambin, L. P. Biro, Tailoring the atomic structure of graphene nanoribbons by scanning tunneling microscope lithography. Nature Nano **3**, 397 (2008).

[11] C. Tao, L. Jiao, O. V. Yazyev, Y.-C. Chen, J. Feng, X. Zhang, R. B. Capaz, J. M. Tour, A. Zettl, S. G. Louie, H. Dai, M. F. Crommie, Spatially resolving edge states of chiral graphene nanoribbons. Nature Phys. **7**, 616 (2011).

[12] Y. Y. Li, M. X. Chen, M. Weinert, L. Li, Direct experimental determination of onset of electron-electron interactions in gap opening of zigzag graphene nanoribbons. Nature Commun. **5**, 4311 (2014).

[13] G. Z. Magda, X. Jin, I. Hagymasi, P. Vancso, Z. Osvath, P. Nemes-Incze, C. Hwang, L. P. Biro, L. Tapaszto, Room-temperature magnetic order on zigzag edges of narrow graphene nanoribbons. Nature **514**, 608 (2014).

[14] J. Hicks, A. Tejeda, A. Taleb-Ibrahimi, M. S. Nevius, F. Wang, K. Shepperd, J. Palmer, F. Bertran, P. Le Fevre, J. Kunc, W. A. de Heer, C. Berger, E. H. Conrad, A wide-bandgap metal-semiconductor-metal nanostructure made entirely from graphene. Nature Phys. **9**, 49 (2013).

[15] J. Baringhaus, M. Ruan, F. Edler, A. Tejeda, M. Sicot, A. Taleb-Ibrahimi, A.-P. Li, Z. Jiang, E. H. Conrad, C. Berger, C. Tegenkamp, W. A. de Heer, Exceptional ballistic transport in epitaxial graphene nanoribbons. Nature **506**, 349 (2014).

[16] I. Palacio, A. Celis, M. N. Nair, A. Gloter, A. Zobelli, M. Sicot, D. Malterre, M. S. Nevius, W. A. de Heer, C. Berger, E. H. Conrad, A. Taleb-Ibrahimi, A. Tejeda, Atomic structure of epitaxial graphene sidewall nanoribbons: flat graphene, miniribbons, and the confinement gap. Nano Lett. **15**, 182 (2015).

[17] A. Kimouche, M. M. Ervasti, R. Drost, S. Halonen, A. Harju, P. M. Joensuu, J. Sainio, P. Liljeroth, Ultra-narrow metallic armchair graphene nanoribbons. Nature Commun. **6**, 10177 (2015).

[18] See Supplemental Material at http://link.aps.org/supplemental/10.1103/PhysRevB.93.241403 for more STM images, STS spectra, and details of the analysis.

[19] D. V. Kosynkin, A. L. Higginbotham, A. Sinitskii, J. R. Lomeda, A. Dimiev, B. K. Price, J. M. Tour, Longitudinal unzipping of carbon nanotubes to form graphene nanoribbons. Nature **458**, 872 (2009).

[20] J. Cai, P. Ruffieux, R. Jaafar, M. Bieri, T. Braun, S. Blankenburg, M. Muoth, A. P. Seitsonen, M. Saleh, X. Feng, K. Mullen, R. Fasel, Atomically precise bottom-up fabrication of graphene nanoribbons. Nature **466**, 470 (2010).

[21] P. Ruffieux, J. Cai, N. C. Plumb, L. Patthey, D. Prezzi, A. Ferretti, E. Molinari, X. Feng, K. Mullen, C. A. Pignedoli, and R. Fasel, Electronic structure of atomically precise graphene nanoribbons. ACS Nano **6**, 6930 (2012).

[22] Y.-C. Chen, D. G. de Oteyza, Zahra Pedramrazi, Chen Chen, Felix R. Fischer and Michael F. Crommie. Tuning the Band gap of graphene nanoribbons synthesized from molecular precursors. ACS Nano **7**, 6123 (2013).

[23] C. Berger, Z. Song, T. Li, X. Li, A. Y. Ogbazghi, R. Feng, Z. Dai, A. N. Marchenkov, E. H. Conrad, P. N. First, W. A. de Heer, Ultrathin epitaxial graphite: 2D electron gas properties and a route toward graphene-based nanoelectronics. J. Phys. Chem. B **108**, 19912 (2004).

[24] X. Wu, X. Li, Z. Song, C. Berger, W. A. de Heer, Weak Antilocalization in Epitaxial Graphene: Evidence for Chiral Electrons. Phys. Rev. Lett. **98**, 136801 (2007).

[25] T. Cai, Z. Jia, B. Yan, D. Yu, X. Wu, Hydrogen assisted growth of high quality epitaxial graphene on the C-face of 4H-SiC. Appl. Phys. Lett. **106**, 013106 (2015).

[26] D. L. Miller, K. D. Kubista, G. M. Rutter, M. Ruan, W. A. de Heer, P. N. First, J. A. Stroscio, Observing the quantization of zero mass carriers in graphene. Science **324**, 924 (2009).

[27] G. Li, A. Luican, E. Y. Andrei, Scanning Tunneling Spectroscopy of Graphene on Graphite. Phys. Rev. Lett. **102**, 176804 (2009).

[28] L.-J. Yin, S.-Y. Li, J.-B. Qiao, J.-C. Nie, L. He, Landau quantization in graphene monolayer, Bernal bilayer, and Bernal trilayer on graphite surface. Phys. Rev. B **91**, 115405 (2015).

[29] W.-X. Wang, L.-J. Yin, J.-B. Qiao, T. Cai, S.-Y. Li, R.-F. Dou, J.-C. Nie, X. Wu, L. He, Atomic resolution imaging of the two-component Dirac-Landau levels in a gapped graphene monolayer. Phys. Rev. B **92**, 165420 (2015).

[30] H. Lim, J. Jung, R. S. Ruoff, Y. Kim, Structurally driven one-dimensional electron confinement in sub-5-nm graphene nanowrinkles, Nature Commun. **6**, 8601 (2015).

[31] D. Gunlycke and C. T. White, Tight-binding energy dispersions of armchair-edge graphene nanostrips. Phys. Rev. B **77**, 115116 (2008).